TRANSACTIONS ON EMERGING TELECOMMUNICATIONS TECHNOLOGIES
Trans. Emerging Tel. Tech. 2015; **26**:380–388
Published online 14 January 2013 in Wiley Online Library (wileyonlinelibrary.com). DOI: 10.1002/ett.2617

RESEARCH ARTICLE

Wireless network coding design based on LDPC codes for a multiple-access relaying system

Jun Li*, Jinhong Yuan and Robert Malaney

School of Electrical Engineering and Telecommunications, University of New South Wales, Sydney, NSW 2052, Australia

ABSTRACT

In this paper, we investigate wireless network coding (WNC) in a multiple-access relay channel (MARC) with two sources, one relay and one destination. We focus on a MARC with binary-input additive white Gaussian noise (AWGN) channels, where two sources' signals interfere at both the relay and the destination. Firstly, we derive the achievable rates for the WNC in the MARC over binary-input AWGN channels. Secondly, considering the strong interference between the two sources, we propose a novel joint WNC and multi-edge type low-density party-check (LDPC) code structure, which we refer to as the WNC–LDPC code. Then, on the basis of our code structure and the iterative receiver at the destination, we optimise the degree distributions of our WNC–LDPC code to approach the achievable sum rate of the MARC by utilising the extrinsic mutual information transfer (EXIT) analysis. In the simulations, we utilise physical-layer network coding (PNC) as a benchmark for comparison purposes and design an LDPC code for the PNC (i.e. PNC–LDPC), which is used to compare with our WNC–LDPC code. Numerical results show that our WNC–LDPC code offers a much better bit error ratio performance relative to the PNC–LDPC code. Copyright © 2013 John Wiley & Sons, Ltd.

***Correspondence**
J. Li, School of Electrical Engineering and Telecommunications, University of New South Wales, Sydney, NSW 2052, Australia.
E-mail: jleesr80@gmail.com

Received 23 March 2012; Revised 24 November 2012; Accepted 16 December 2012

1. INTRODUCTION

In a multiple-access relay channel (MARC) with multiple sources, one relay and one destination, the sources transmit to their common destination simultaneously with the help of the relay. Conventional decode-and-forward (DF) protocols of the classic relay channels [1] can be readily extended to the MARC, and the capacity outer bound and the achievable rate region of the Gaussian input MARC with the DF protocol have been well investigated in [2]. In a DF-based MARC, the achievable rate region of the MARC is the intersection between the rate region of the source-to-relay multiple-access channel (MAC) and the rate region of the source-and-relay-to-destination MAC [2].

Wireless network coding (WNC) combined with a powerful channel code is an effective method to approach the achievable rates of the DF-based multi-source relaying systems [3–8]. In these network coding schemes, the relay explicitly decodes the messages of each source and combines these messages on the basis a channel code to obtain network-coded parity check digits. However, in these multi-source relaying systems, all the sources are supposed to transmit in orthogonal channels. When optimising the codes, the works in [5–8] have not considered the multi-source interference, which simplifies the code design. In [9], the authors consider three relaying strategies for a two-source MARC. However, they do not consider the joint channel-network code optimisation to approach the system's achievable rates.

Physical-layer network coding (PNC) [10, 11], on the other hand, is proposed in a two-way relay channel to enhance the error performance of the source-to-relay MAC. Compared with the WNC (where explicit decoding of each source's message is performed at the relay), the main property of PNC is that in PNC, the relay only needs to decode and forward the codeword-wise-XOR results of all the sources' messages. This means that the relay does not have to explicitly decode each source's message. Because of this partial decoding of PNC at the relay, the bit error ratio (BER) of PNC can outperform that of the WNC in a two-way relay channel. However, in MARC, this is not the case. This is because in PNC, (1) all the sources must transmit their messages by using the same channel code, and (2) the relay only forwards the codeword-wise-XOR results of all the sources' messages for the decoding at the destination. In an MARC with PNC, these two constraints of the PNC lead to the fact that when decoding at the destination, the parity checks from the relay cannot provide the sources with much useful extrinsic mutual information. Therefore, the error performance of the PNC scheme could be poor in the MARC.

In this paper, we consider a binary-input additive white Gaussian noise (BIAWGN) MARC with two sources and one half-duplexing relay. We focus on a strong interference scenario where the two sources transmit simultaneously and have the same distance to the relay. We are interested in the design of joint WNC and multi-edge type low-density party-check (LDPC) codes [12] (WNC–LDPC) for the MARC under strong interference. Our contributions are as follows. (1) We investigate the achievable rates of the BIAWGN MARC. (2) We propose a novel joint WNC and multi-edge type LDPC code structure. (3) We optimise the WNC–LDPC code to approach the achievable sum rate by utilising the extrinsic mutual information transfer (EXIT) analysis [13, 14]. In the BER simulations, we utilise a PNC-based LDPC (PNC–LDPC) code as a benchmark. Numerical results show that the BER performance of our WNC–LDPC code is much better than the PNC–LDPC code because PNC–LDPC code cannot converge for the whole signal-to-noise ratio (SNR) region.

The rest of this paper is organised as follows. Section 2 sets up the system model of the MARC. Section 3 presents the achievable rate analysis of the MARC with the WNC. In Section 4, we propose the structure of the WNC–LDPC codes and optimise the WNC–LDPC codes by an EXIT analysis. Section 5 provides our simulation results, and Section 6 concludes the paper.

2. SYSTEM MODEL

We consider an MARC system with two sources, one relay and one destination. Figure 1 shows the channel model. The two sources, $\mathcal{S}_1$ and $\mathcal{S}_2$, transmit their information to the common destination $\mathcal{D}$ with the help of a half-duplexing relay $\mathcal{R}$. The two sources are randomly located on a circle around the relay with the angles φ_1 and φ_2 (uniformly distributed in $(0, 2\pi]$), respectively. The distance between $\mathcal{S}_i$ and the relay $\mathcal{R}$ is denoted as $d_\mathcal{R}$, the distance between the relay $\mathcal{R}$ and the destination $\mathcal{D}$ is $d_{\mathcal{R}\mathcal{D}}$, and the distance between $\mathcal{S}_i$ and the destination $\mathcal{D}$ is $d_{i\mathcal{D}}$. The pass losses of all the channels are related to their distances with the attenuation exponent γ. Therefore, the channel coefficients between $\mathcal{S}_i$ and $\mathcal{R}$, $\mathcal{S}_i$ and $\mathcal{D}$, and $\mathcal{R}$ and $\mathcal{D}$ are calculated as $h_\mathcal{R} = 1/\sqrt{(d_\mathcal{R})^\gamma}$, $h_{i\mathcal{D}} = 1/\sqrt{(d_{i\mathcal{D}})^\gamma}$ and $h_{\mathcal{R}\mathcal{D}} = 1/\sqrt{(d_{\mathcal{R}\mathcal{D}})^\gamma}$, respectively.

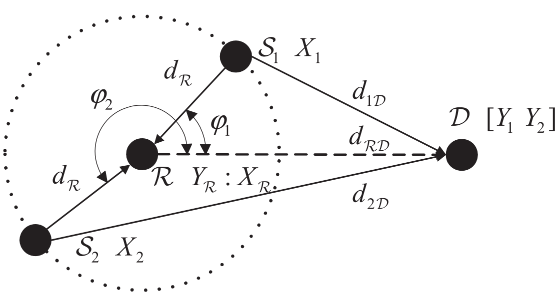

Figure 1. The system model of the MARC with two sources, one relay and one destination. The arrows with solid lines represent the first transmission phase, and the arrow with dashed line represents the second transmission phase.

We split one transmission period (n time slots) into two phases. The first phase is composed of tn time slots $(0 < t < 1)$, in which the two sources simultaneously broadcast their channel-encoded codewords $\mathbf{X}_1$ and $\mathbf{X}_2$, respectively, to both the destination and the relay. The second phase is composed of $(1-t)n$ time slots, in which the two sources keep silent while the relay generates the extra redundant message of the two sources and forwards the channel-encoded codeword $\mathbf{X}_\mathcal{R}$ to the destination so as to facilitate the decoding process. In the first phase, the signals received by the destination and the relay are denoted as $\mathbf{Y}_1$ and $\mathbf{Y}_\mathcal{R}$, respectively, whereas in the second phase, the signal received at the destination is denoted as $\mathbf{Y}_2$. After the second phase, the destination decodes the information of the sources by combining the received signals of the two phases.

To normalise the transmission power, we assume that both sources have the same transmission power of one and that the relay has the transmission power of two. We assume that the transmitted codewords $\mathbf{X}_i$, $i = 1, 2$ and $\mathbf{X}_\mathcal{R}$ are modulated with binary phase-shift keying (BPSK) signals. We have $\mathbf{X}_i = \left[x_i^1, \ldots, x_i^{tn}\right]^T$, where $x_i^j \in \{-1, +1\}$, $j = 1, \ldots, tn$, is a BPSK symbol, and $\mathbf{X}_\mathcal{R} = \left[x_\mathcal{R}^1, \ldots, x_\mathcal{R}^{(1-t)n}\right]^T$, where $x_\mathcal{R}^{j'} \in \{-\sqrt{2}, +\sqrt{2}\}$, $j' = 1, \ldots, (1-t)n$, is a BPSK symbol. All the symbols are independent and identically distributed; that is, for each symbol, we have the probability $P(x_i^j) = 0.5$. Suppose that all the information is encoded by systematic linear channel codes. The information part of $\mathbf{X}_i$ is denoted as $\bar{\mathbf{X}}_i = \left[x_i^1, \ldots, x_i^{tnR_i}\right]^T$, where R_i is $\mathcal{S}_i$'s code rate. The information part of $\mathbf{X}_\mathcal{R}$ is denoted as $\bar{\mathbf{X}}_\mathcal{R} = \left[x_\mathcal{R}^1, \ldots, x_\mathcal{R}^{(1-t)nR_\mathcal{R}}\right]^T$, where $R_\mathcal{R}$ is the relay's code rate. The information part of $\mathbf{X}_\mathcal{R}$, that is, $\bar{\mathbf{X}}_\mathcal{R}$, is the network-coded parity check digits generated by the relay. These digits are generated on the basis of the codewords of the two sources. Then, $\bar{\mathbf{X}}_\mathcal{R}$ is encoded into $\mathbf{X}_\mathcal{R}$ by a channel code of the relay with the rate $R_\mathcal{R}$ before transmission. In the code design, we assume that $\bar{\mathbf{X}}_\mathcal{R}$ is encoded by a desired channel code and can be perfectly decoded from $\mathbf{Y}_2$ at the destination if $R_\mathcal{R} \leqslant \frac{I(\mathbf{X}_\mathcal{R};\mathbf{Y}_2)}{(1-t)n}$. All the channels are AWGN distributed, and all the receivers have the noise power σ^2. We can write the received signals at the relay and the destination as $\mathbf{Y}_\mathcal{R} = h_\mathcal{R}(\mathbf{X}_1 + \mathbf{X}_2) + \mathbf{N}_\mathcal{R}$, $\mathbf{Y}_1 = h_{1\mathcal{D}}\mathbf{X}_1 + h_{2\mathcal{D}}\mathbf{X}_2 + \mathbf{N}_1$ and $\mathbf{Y}_2 = h_{\mathcal{R}\mathcal{D}}\mathbf{X}_\mathcal{R} + \mathbf{N}_2$, respectively, where $\mathbf{N}_\mathcal{R}$ is the noise observed by the relay, and $\mathbf{N}_1$ and $\mathbf{N}_2$ are the noises observed by the destination in the first and second phases, respectively.

3. ACHIEVABLE RATES ANALYSIS

We now consider the achievable rates of the WNC under the BIAWGN MARC. The relay needs to fully decode information from two sources. According to [2], the achievable rate region of the DF-based MARC is the intersection between the rate region of the source-to-relay MAC and the rate region of the source-and-relay-to-destination MAC. As such, the achievable rate region of the WNC can be written as

$$\begin{aligned} R_1^{Ac} &\leqslant \frac{1}{n}\cdot \\ &\min\{I(\mathbf{X}_1;\mathbf{Y}_{\mathcal{R}}|\mathbf{X}_2), I(\mathbf{X}_1;\mathbf{Y}_1|\mathbf{X}_2)+I(\mathbf{X}_{\mathcal{R}};\mathbf{Y}_2)\}, \\ R_2^{Ac} &\leqslant \frac{1}{n}\cdot \\ &\min\{I(\mathbf{X}_2;\mathbf{Y}_{\mathcal{R}}|\mathbf{X}_1), I(\mathbf{X}_2;\mathbf{Y}_1|\mathbf{X}_1)+I(\mathbf{X}_{\mathcal{R}};\mathbf{Y}_2)\}, \\ R_1^{Ac}+R_2^{Ac} &\leqslant \frac{1}{n}\cdot \\ &\min\{I(\mathbf{X}_1,\mathbf{X}_2;\mathbf{Y}_{\mathcal{R}}), I(\mathbf{X}_1,\mathbf{X}_2;\mathbf{Y}_1)+I(\mathbf{X}_{\mathcal{R}};\mathbf{Y}_2)\} \end{aligned} \tag{1}$$

The calculations of all the mutual information are based on the BIAWGN channels [13]. The mutual information $I(\mathbf{X}_1;\mathbf{Y}_{\mathcal{R}}|\mathbf{X}_2)$, $I(\mathbf{X}_2;\mathbf{Y}_{\mathcal{R}}|\mathbf{X}_1)$, $I(\mathbf{X}_1;\mathbf{Y}_1|\mathbf{X}_2)$, $I(\mathbf{X}_2;\mathbf{Y}_1|\mathbf{X}_1)$ and $I(\mathbf{X}_{\mathcal{R}};\mathbf{Y}_2)$ in Equation (1) can be calculated as that of the single-link BIAWGN channels. However, the derivations of the mutual information $\frac{1}{nt}I(\mathbf{X}_1,\mathbf{X}_2;\mathbf{Y}_{\mathcal{R}})$ and the mutual information $\frac{1}{nt}I(\mathbf{X}_1,\mathbf{X}_2;\mathbf{Y}_1)$ are not straightforward. Without loss of generality, we focus on the calculation of $\frac{1}{nt}I(\mathbf{X}_1,\mathbf{X}_2;\mathbf{Y}_{\mathcal{R}})$.

We pick out the jth symbol of $\mathbf{X}_i$, that is, x_i^j, and then, we have $y_1^j = h_{1\mathcal{D}}x_1^j + h_{2\mathcal{D}}x_2^j + n_1^j$, where y_1^j and n_1^j are the jth samples of $\mathbf{Y}_1$ and $\mathbf{N}_1$, respectively. We have $I\left(x_1^j, x_2^j; y_1^j\right) = \frac{1}{nt}I(\mathbf{X}_1,\mathbf{X}_2;\mathbf{Y}_1)$. The conditional probability density function belonging to y_1^j can be written as

$$\begin{aligned} &p\left(y_1^j|x_1^j,x_2^j\right) \\ &= \frac{1}{\sqrt{2\pi}\sigma}\exp\left\{-\frac{\left(y_1^j-h_{1\mathcal{D}}x_1^j-h_{2\mathcal{D}}x_2^j\right)^2}{2\sigma^2}\right\} \end{aligned} \tag{2}$$

Note that $I\left(x_1^j, x_2^j; y_1^j\right)$ is calculated as

$$\begin{aligned} I\left(x_1^j,x_2^j;y_1^j\right) &= \sum_{x_1^j=\pm 1}\sum_{x_2^j=\pm 1} \\ &\int_{-\infty}^{\infty} p\left(x_1^j,x_2^j,y_1^j\right)\log\frac{p\left(y_1^j|x_1^j,x_2^j\right)}{p\left(y_1^j\right)}\,dy_1^j \end{aligned} \tag{3}$$

Because all the transmitted symbols are independent and identically distributed, we have the probability $P\left(x_1^j=u,x_2^j=v\right) = P\left(x_1^j=u\right)P\left(x_2^j=v\right) = \frac{1}{4}$, $u,v\in\{-1,1\}$. Also note that $p\left(x_1^j=u,x_2^l=v,y_1^j\right) = \frac{1}{4}p\left(y_1^j|x_1^j=u,x_2^l=v\right)$ and

$$\begin{aligned} p\left(y_1^j\right) &= \sum_{u=\pm 1}\sum_{v=\pm 1} \\ &\quad p\left(y_1^j|x_1^j=u,x_2^j=v\right)P\left(x_1^j=u,x_2^j=v\right) \\ &= \frac{1}{4}\sum_{u=\pm 1}\sum_{v=\pm 1} p\left(y_1^j|x_1^j=u,x_2^j=v\right) \end{aligned} \tag{4}$$

Then, we rewrite $I\left(x_1^j,x_2^j;y_1^j\right)$ as

$$\begin{aligned} &I\left(x_1^j,x_2^j;y_1^j\right) \\ &= \frac{1}{4}\sum_{u=\pm 1}\sum_{v=\pm 1}\int_{-\infty}^{\infty} p\left(y_1^j|x_1^j=u,x_2^j=v\right) \\ &\log\frac{4p\left(y_1^j|x_1^j=u,x_2^j=v\right)}{\sum\limits_{u_1=\pm 1}\sum\limits_{v_1=\pm 1} p\left(y_1^j|x_1^j=u_1,x_2^j=v_1\right)}\,dy_1^j \end{aligned} \tag{5}$$

Following the same method, we can obtain $\frac{1}{nt}I(\mathbf{X}_1,\mathbf{X}_2;\mathbf{Y}_{\mathcal{R}})$ in the source-to-relay MAC.

4. WNC–LDPC CODE STRUCTURE AND OPTIMISATION

4.1. Code structure

We utilise a multi-edge type structure [12] to represent a WNC–LDPC code. Before we represent the WNC–LDPC code using the multi-edge type structure, we firstly introduce the definitions and notations of the multi-edge type structure. The multi-edge type ensemble can be specified through two polynomials; one is associated with variable nodes, and the other is associated with check nodes. The polynomials are given by

$$v(\mathbf{r},\mathbf{w}) = \sum v_{\mathbf{b},\mathbf{d}}\mathbf{r}^{\mathbf{b}}\mathbf{w}^{\mathbf{d}} \quad \text{and} \quad \mu(\mathbf{w}) = \sum \mu_{\mathbf{d}}\mathbf{w}^{\mathbf{d}} \tag{6}$$

where $\mathbf{d} = [d_1, d_2, \ldots, d_{n_\varsigma}]$ is the *edge degree vector* of length n_ς and $\mathbf{b} = [b_0, b_1, \ldots, b_{n_\tau}]$ is the *received degree vector* of length $n_\tau + 1$. Note that in vector $\mathbf{b}$, the first element b_0 is utilised to indicate punctured variable nodes. We denote n_ς as the number of edge types used in the graph's ensemble and n_τ as the number of different channels over which a bit may be transmitted. The vector of variables is denoted by $\mathbf{w} = [w_1, \ldots, w_{n_\varsigma}]$, whereas the vector of variables corresponding to the received distributions is denoted by $\mathbf{r} = [r_0, r_1, \ldots, r_{n_\tau}]$. Here, we have $\mathbf{w}^{\mathbf{d}} = \prod_{\iota=1}^{n_\varsigma} w_\iota^{d_\iota}$ and $\mathbf{r}^{\mathbf{b}} = \prod_{\iota=0}^{n_\tau} r_\iota^{b_\iota}$. The coefficients $v_{\mathbf{b},\mathbf{d}}$ and $\mu_{\mathbf{d}}$ are non-negative reals, which correspond to the percentage of variable nodes with type ($\mathbf{b}$, $\mathbf{d}$) and check nodes

Trans. Emerging Tel. Tech. **26**:380–388 (2015) © 2013 John Wiley & Sons, Ltd.
DOI: 10.1002/ett

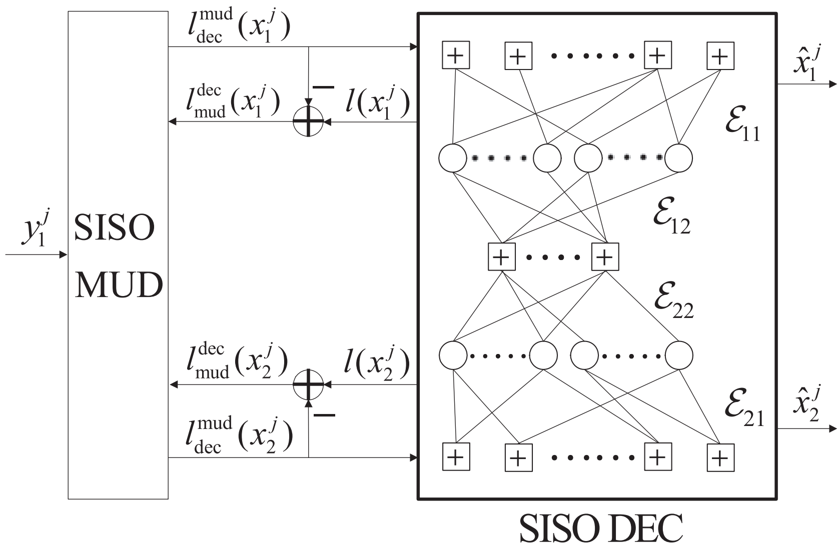

Figure 2. Iterative receiver structure at the destination. The receiver is composed of a soft-in-soft-out (SISO) multi-user detector (MUD) and an SISO decoder (DEC). The Tanner graph of the WNC–LDPC code is illustrated in the DEC.

with type (**d**), respectively. More details on multi-edge type LDPC codes are given in [12].

According to the design of bilayer multi-edge type LDPC codes in the single-source relaying channels [15], we use four edge types to represent the WNC–LDPC code structure as shown in Figure 2. For the source $\mathcal{S}_i$, we have two edge types (i.e. $\mathcal{E}_{i1}$ and $\mathcal{E}_{i2}$). In the WNC–LDPC code design, we firstly fix the codes for the source-to-relay MAC, which is represented by the edge type $\mathcal{E}_{i1}$. Then, with the $\mathcal{E}_{i1}$, we design the code to generate the network-coded digits at the relay, which is represented by the edge type $\mathcal{E}_{i2}$. To implement the code in the MARC, we first obtain the degree distributions of $\mathcal{E}_{i1}$ for S_i and $i = 1, 2$, which are optimised for the source-to-relay channels. Based on the degree distributions of $\mathcal{E}_{11}$ and $\mathcal{E}_{21}$, we further optimise the degree distributions of $\mathcal{E}_{12}$ and $\mathcal{E}_{22}$.

Next, we assign the structure of the WNC–LDPC code with two types of the received degree (i.e. $n_\tau = 2$). This is because the codewords $\mathbf{X}_1$ and $\mathbf{X}_2$ experience two different source-to-destination channels. With four different edge types and two types of received degree, the polynomials for WNC–LDPC code can be written as

$$\begin{aligned} v(\mathbf{r}, \mathbf{w}) &= r_1 \sum_{a=1}^{d_{v,1}} \sum_{b=0}^{d_{v,2}} v_{[0,1,0],[a,b,0,0]} w_1^a w_2^b \\ &\quad + r_2 \sum_{c=1}^{d_{v,3}} \sum_{d=0}^{d_{v,4}} v_{[0,0,1],[0,0,c,d]} w_3^c w_4^d \\ \mu(\mathbf{w}) &= \sum_{a=1}^{d_{c,1}} \mu_{[a,0,0,0]} w_1^a + \sum_{c=1}^{d_{c,3}} \mu_{[0,0,c,0]} w_3^c \\ &\quad + \sum_{b=1}^{d_{c,2}} \sum_{d=1}^{d_{c,4}} \mu_{[0,b,0,d]} w_2^b w_4^d \end{aligned} \tag{7}$$

where r_1 and r_2 denote the variable nodes associated with $\mathbf{X}_1$ and $\mathbf{X}_2$, respectively. More specifically, r_1 and r_2 are associated with the $\mathcal{S}_1$-to-destination channel and the $\mathcal{S}_2$-to-destination channel, respectively. The variable nodes transmitted in the $\mathcal{S}_i$-to-destination channel (i.e. the symbols in $\mathbf{X}_i$) are connected to the edge types $\mathcal{E}_{i1}$ and $\mathcal{E}_{i2}$. The edge degree vector $\mathbf{d} = [a, b, c, d]$ represents four types of edge degree with a, b, c and d denoting the variable or check nodes' degrees of the edge types $\mathcal{E}_{11}$, $\mathcal{E}_{12}$, $\mathcal{E}_{21}$ and $\mathcal{E}_{22}$, respectively.

4.2. Iterative receiver

The WNC–LDPC codes are optimised on the basis of both the code structure and the iterative receiver structure at the destination. Figure 2 shows the receiver structure and the Tanner graph of the code structure. In Figure 2, there are a soft-in-soft-out (SISO) multi-user detector (MUD) and an SISO belief propagation (BP) decoder (denoted as DEC). The extrinsic log-likelihood ratios (LLRs) are exchanged between the MUD and the DEC in each iteration. Specifically, the MUD utilises the input LLRs $l_{\text{mud}}^{\text{dec}}\left(x_1^j\right)$ and $l_{\text{mud}}^{\text{dec}}\left(x_2^j\right)$ to update its output LLRs $l_{\text{dec}}^{\text{mud}}\left(x_1^j\right)$ and $l_{\text{dec}}^{\text{mud}}\left(x_2^j\right)$, where the LLR $l_{\text{mud}}^{\text{dec}}\left(x_i^j\right)$ is defined as $\ln\left(P\left(x_i^j = 1\right) / \left(x_i^j = -1\right)\right)$. Without loss of generality, we focus on the LLR $l_{\text{dec}}^{\text{mud}}\left(x_1^j\right)$, which is shown in Equation (8). In Equation (8), the original value of the probabilities $P\left(x_i^j = 1\right)$ and $P\left(x_i^j = -1\right)$ is 0.5, and the conditional probability density function $p\left(y_1^j | x_1^j, x_2^j\right)$ is shown in Equation (2). In the MUD, we use the extrinsic LLR $l_{\text{mud}}^{\text{dec}}\left(x_2^j\right)$ to update the probability $P\left(x_2^j\right)$ in $l_{\text{dec}}^{\text{mud}}\left(x_1^j\right)$

and use the extrinsic LLR $l_{\text{mud}}^{\text{dec}}\left(x_1^j\right)$ to update the probability $P\left(x_1^j\right)$ in $l_{\text{dec}}^{\text{mud}}\left(x_2^j\right)$ in each iteration. The probability $P\left(x_i^j\right)$ is updated as

$$l_{\text{dec}}^{\text{mud}}\left(x_1^j\right) = \ln\left(\frac{p\left(y_1^j|x_1^j=1,x_2^j=1\right)P\left(x_1^j=1\right)P\left(x_2^j=1\right)+p\left(y_1^j|x_1^j=1,x_2^j=-1\right)P\left(x_1^j=1\right)P\left(x_2^j=-1\right)}{p\left(y_1^j|x_1^j=-1,x_2^j=1\right)P\left(x_1^j=-1\right)P\left(x_2^j=1\right)+p\left(y_1^j|x_1^j=-1,x_2^j=-1\right)P\left(x_1^j=-1\right)P\left(x_2^j=-1\right)}\right) \tag{8}$$

$$\begin{aligned} P\left(x_i^j=1\right) &= \frac{\exp\left(l_{\text{mud}}^{\text{dec}}\left(x_i^j\right)\right)}{1+\exp\left(l_{\text{mud}}^{\text{dec}}\left(x_i^j\right)\right)} \\ P\left(x_i^j=-1\right) &= \frac{1}{1+\exp\left(l_{\text{mud}}^{\text{dec}}\left(x_i^j\right)\right)} \end{aligned} \tag{9}$$

From the DEC point of view, $l_{\text{dec}}^{\text{mud}}\left(x_1^j\right)$ and $l_{\text{dec}}^{\text{mud}}\left(x_2^j\right)$ are utilised as the extrinsic channel LLRs. BP decoding is applied to the parity check matrix of the WNC–LDPC code. Joint decoding of the two sources' codewords is enabled by the network-coded parity checks transmitted from the relay. We denote the output LLR of the DEC as $l(x_i^j)$. As shown in Figure 2, to make the input LLR of the MUD, that is, $l_{\text{mud}}^{\text{dec}}\left(x_i^j\right)$, to be extrinsic, we calculate it as $l_{\text{mud}}^{\text{dec}}\left(x_i^j\right) = l\left(x_i^j\right) - l_{\text{dec}}^{\text{mud}}\left(x_i^j\right)$.

4.3. Code optimisation

Here, code optimisation means the optimisation method to obtain a good code profile with a given code rate. We note that the LDPC code design for a two-user MAC has been studied in [16]. Here, we will fix the LDPC codes for the source-to-relay MAC according to [16] and then optimise the network code at the relay. Because of the interference of the two sources at the destination, the input LLR of the DEC $l_{\text{dec}}^{\text{mud}}\left(x_i^j\right)$ is composed of two different conditional LLR values. We focus on $x_1^j = 1$. The two conditional LLR values of x_1^j correspond to the two cases when $x_2^j = 1$ and $x_2^j = -1$, respectively. We denote the two conditional LLR values as $l_{\text{dec}}^{\text{mud}}\left(x_1^j|x_2^j=1\right)$ and $l_{\text{dec}}^{\text{mud}}\left(x_1^j|x_2^j=-1\right)$, which can be modelled as two Gaussian variables with different means and variances. In the kth iteration between the MUD and the DEC, we denote the variance of $l_{\text{dec}}^{\text{mud}}\left(x_1^j|x_2^j=1\right)$ and $l_{\text{dec}}^{\text{mud}}\left(x_1^j|x_2^j=-1\right)$ as $\left(\sigma_{1|+1,+1}^{(k)}\right)^2$ and $\left(\sigma_{1|+1,-1}^{(k)}\right)^2$, respectively.

Now, we optimise the WNC–LDPC code by EXIT analysis [13, 14]. To track the extrinsic mutual information inside of the DEC, we denote $I_{Ev,il|+1,+1}^{(k,q)}$, $l = 1, 2$, as the averaged conditional extrinsic mutual information $\left(\text{on the condition that } x_1^j = 1, \text{and } x_2^j = 1\right)$ sent along the edge type $\mathcal{E}_{il}$ from the variable nodes to the check nodes in the qth iteration of the BP decoding and the kth iteration between the MUD and the DEC. Similarly, when $x_1^j = 1$ and $x_2^j = -1$, we obtain the averaged conditional extrinsic mutual information $I_{Ev,il|+1,-1}^{(k,q)}$. We denote $I_{Ec,il}^{(k,q)}$ as the averaged extrinsic mutual information sent on the edge type $\mathcal{E}_{il}$ from the check nodes to the variable nodes in the qth iteration of the BP decoding and the kth iteration between the MUD and the DEC. Also, note that the extrinsic mutual information on an edge connecting the variable nodes to the check nodes, at the output of the variable nodes, is the *a-priori* mutual information for the check nodes in the current iteration of BP decoding, that is, $I_{Ac,il|+1,+1}^{(k,q)} = I_{Ev,il|+1,+1}^{(k,q)}$ and $I_{Ac,il|+1,-1}^{(k,q)} = I_{Ev,il|+1,-1}^{(k,q)}$. Similarly, the extrinsic mutual information on an edge connecting the check nodes to the variable nodes, at the output of the check node, is the *a-priori* mutual information for the variable nodes in the next iteration of BP decoding, that is, $I_{Av,il}^{(k,q+1)} = I_{Ec,il}^{(k,q)}$. We use the $J(\cdot)$ function [13] to represent the mutual information of a single-link BIAWGN channel. Firstly, we track the extrinsic mutual information from the variable nodes to the check nodes, at the output of the variable nodes. For the variable nodes in $\mathcal{S}_1$, we have the mutual information as shown in Equation (10). Note that in Equation (10), $\lambda_{[a,b,0,0]}^{(a)} = \frac{v_{[0,1,0],[a,b,0,0]}a}{\sum_{a'=1}^{d_{v,1}}\sum_{b'=1}^{d_{v,2}} v_{[0,1,0],[a',b',0,0]}a'}$ and $\lambda_{[a,b,0,0]}^{(b)} = \frac{v_{[0,1,0],[a,b,0,0]}b}{\sum_{a'=1}^{d_{v,1}}\sum_{b'=1}^{d_{v,2}} v_{[0,1,0],[a',b',0,0]}b'}$. Similarly, we can obtain $I_{Ev,2l|+1,+1}^{(k,q)}$ and $I_{Ev,2l|+1,-1}^{(k,q)}$ for $\mathcal{S}_2$. Then, we track the extrinsic mutual information from the check nodes to the variable nodes, at the output of the check nodes. For the check nodes in $\mathcal{S}_1$, we have the mutual information shown in Equation (11). Note that in Equation (11), $\rho_{[a,0,0,0]}^{(a)} = \frac{\mu_{[a,0,0,0]}a}{\sum_{a'=1}^{d_{c,1}}\mu_{[a',0,0,0]}a'}$ and $\rho_{[0,b,0,d]}^{(b)} = \frac{\mu_{[0,b,0,d]}b}{\sum_{b'=1}^{d_{c,2}}\sum_{d'=1}^{d_{v,4}}\mu_{[0,b',0,d']}b'}$. In Equation (11), the coefficient $\left(\frac{a-1}{2}\right)$ $\left(\text{or}\left(\frac{b-1}{2}\right)\right)$ means that within $(a-1)$ (or $(b-1)$) edges that are respectively connected to $a-1$ variable node, there are average 50% edges connected to the received symbol pairs $\left(x_1^j = 1, x_2 = 1\right)$ or $\left(x_1^j = -1, x_2 = -1\right)$, and the other 50% edges connected

Trans. Emerging Tel. Tech. **26**:380–388 (2015) © 2013 John Wiley & Sons, Ltd.
DOI: 10.1002/ett

to the received symbol pairs ($x_1 = 1, x_2 = -1$) or ($x_1 = -1, x_2 = 1$). This means that there are average 50% edges with the extrinsic mutual information $I_{Ev,1l|+1,+1}$ (because $I_{Ev,1l|+1,+1}$=$I_{Ev,1l|-1,-1}$) and the other 50% edges with the extrinsic mutual information $I_{Ev,1l|+1,-1}$ (because $I_{Ev,1l|+1,-1}$=$I_{Ev,1l|-1,+1}$). Similarly, we can obtain $I^{(k,q)}_{Ec,2l}$ for $\mathcal{S}_2$.

power, the same rate and the same distance to the destination and to the relay as well. Therefore, we have the strongest sources interference when optimising the code. Note that the code optimisation for asymmetric models (e.g. different code rates and different source-to-destination distances) will be easier than the symmetric model. We assume that $\varphi_1 = \varphi_2 = \pi$. The distance between each source and the relay is $d_{\mathcal{R}} = 0.5$. The distance between the relay and the destination is $d_{\mathcal{RD}} = 0.5$. The distance between $\mathcal{S}_i$ and the destination is $d_{i\mathcal{D}} = 1$. The channel attenuation exponents are all $\gamma = 2$. The transmission SNR in all the simulations is defined as the transmission SNR of each source $\left(\text{i.e.} \frac{1}{\sigma^2}\right)$.

$$
\begin{aligned}
I^{(k,q)}_{Ev,11|+1,+1} &= \sum_{a=1}^{d_{v,1}} \sum_{b=1}^{d_{v,2}} J\left(\sqrt{(a-1)\left(J^{-1}\left(I^{(k,q)}_{Av,11}\right)\right)^2 + b\left(J^{-1}\left(I^{(k,q)}_{Av,12}\right)\right)^2 + \left(2/\sigma^{(k)}_{1|+1,+1}\right)^2}\right)\lambda^{(a)}_{[a,b,0,0]} \\
I^{(k,q)}_{Ev,11|+1,-1} &= \sum_{a=1}^{d_{v,1}} \sum_{b=1}^{d_{v,2}} J\left(\sqrt{(a-1)\left(J^{-1}\left(I^{(k,q)}_{Av,11}\right)\right)^2 + b\left(J^{-1}\left(I^{(k,q)}_{Av,12}\right)\right)^2 + \left(2/\sigma^{(k)}_{1|+1,-1}\right)^2}\right)\lambda^{(a)}_{[a,b,0,0]} \\
I^{(k,q)}_{Ev,12|+1,+1} &= \sum_{a=1}^{d_{v,1}} \sum_{b=1}^{d_{v,2}} J\left(\sqrt{a\left(J^{-1}\left(I^{(k,q)}_{Av,11}\right)\right)^2 + (b-1)\left(J^{-1}\left(I^{(k,q)}_{Av,12}\right)\right)^2 + \left(2/\sigma^{(k)}_{1|+1,+1}\right)^2}\right)\lambda^{(b)}_{[a,b,0,0]} \\
I^{(k,q)}_{Ev,12|+1,-1} &= \sum_{a=1}^{d_{v,1}} \sum_{b=1}^{d_{v,2}} J\left(\sqrt{a\left(J^{-1}\left(I^{(k,q)}_{Av,11}\right)\right)^2 + (b-1)\left(J^{-1}\left(I^{(k,q)}_{Av,12}\right)\right)^2 + \left(2/\sigma^{(k)}_{1|+1,-1}\right)^2}\right)\lambda^{(b)}_{[a,b,0,0]}
\end{aligned}
\tag{10}
$$

$$
\begin{aligned}
I^{(k,q)}_{Ec,11} &= 1 - \sum_{a=1}^{d_{c,1}} J\left(\sqrt{\frac{a-1}{2}\left(J^{-1}\left(1-I^{(k,q)}_{Ac,11|+1,+1}\right)\right)^2 + \frac{a-1}{2}\left(J^{-1}\left(1-I^{(k,q)}_{Ac,11|+1,-1}\right)\right)^2}\right)\rho^{(a)}_{[a,0,0,0]} \\
I^{(k,q)}_{Ec,12} &= 1 - \sum_{b=1}^{d_{c,2}}\sum_{d=1}^{d_{c,4}} J\left(\sqrt{\frac{b-1}{2}\left(J^{-1}\left(1-I^{(k,q)}_{Ac,12|+1,+1}\right)\right)^2 + \frac{b-1}{2}\left(J^{-1}\left(1-I^{(k,q)}_{Ac,12|+1,-1}\right)\right)^2 +}\right. \\
&\qquad \left.\overline{\frac{d}{2}\left(J^{-1}\left(1-I^{(k,q)}_{Ac,22|+1,+1}\right)\right)^2 + \frac{d}{2}\left(J^{-1}\left(1-I^{(k,q)}_{Ac,22|+1,-1}\right)\right)^2}\right)\rho^{(b)}_{[0,b,0,d]}
\end{aligned}
\tag{11}
$$

We assume that the receiver at the destination conducts total K iterations between the MUD and the DEC. In each iteration between the MUD and the DEC, the DEC conducts Q decoding iterations. At the end of all the iterations, the receiver will make hard decisions based on the output of the DEC. To successfully decode both sources' information, we ensure that $I^{(K,Q)}_{Ev,il|+1,+1} \to 1$ and $I^{(K,Q)}_{Ev,il|+1,-1} \to 1$ for all $i, l = 1, 2$. Given these requirements, we optimise the code by searching a code profile with the maximum threshold σ. Because the optimisation of the degree distribution is a multiple-object optimisation, we use the differential evolution method to solve the optimisation problem. For more details about the differential evolution, please refer to [17].

5. NUMERICAL RESULTS

We consider a symmetric MARC in the simulation, where the interference between the two sources are the most severe; that is, we assume both sources have the same

Figure 3 shows various mutual information and time allocation in the MARC. We can see that when the SNR is large enough, say 10 dB, the achievable sum rate of the source-to-relay MAC, that is, $\frac{1}{nt} I(\mathbf{X}_1, \mathbf{X}_2; \mathbf{Y}_{\mathcal{R}})$, approaches 1.5, and the achievable sum rate of the source-to-destination MAC, i.e. $\frac{1}{nt} I(\mathbf{X}_1, \mathbf{X}_2; \mathbf{Y}_1)$ approaches 1.5. The mutual information $\frac{1}{nt} I(\mathbf{X}_i; \mathbf{Y}_{\mathcal{R}}|\mathbf{X}_j)$, approaches one. Also, the mutual information $\frac{1}{nt} I(\mathbf{X}_i; \mathbf{Y}_1|\mathbf{X}_j)$ approaches one. The relay-to-destination channel is a single-link BIAWGN channel, in which the achievable rate, that is, $\frac{1}{(1-t)n} I(\mathbf{X}_{\mathcal{R}}; \mathbf{Y}_2)$, approaches one at 10 dB. Figure 3 also shows the optimal time allocations at difference SNR values. The optimal time allocation t is calculated by letting $I(\mathbf{X}_1, \mathbf{X}_2; \mathbf{Y}_{\mathcal{R}}) = I(\mathbf{X}_1, \mathbf{X}_2; \mathbf{Y}_1) + I(\mathbf{X}_{\mathcal{R}}; \mathbf{Y}_2)$ in Equation (1). The system achievable rate of

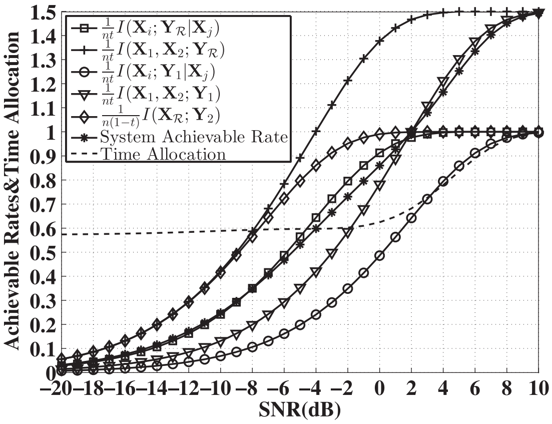

Figure 3. Achievable rates in the multiple-access relay channel with the wireless network coding. SNR, signal-to-noise ratio.

the MARC can be determined on the basis of the optimal time allocation, which is also shown in Figure 3.

In the code design, the sum code rate of S_i and S_j are designed to be equal to the achievable sum rate in the source-to-relay MAC, that is, $\frac{1}{nt}I(\mathbf{X}_1,\mathbf{X}_2;\mathbf{Y}_\mathcal{R})$. Also, the relay's code rate is designed to be equal to the achievable rate of the relay-to-destination channel, that is, $\frac{1}{(1-t)n}I(\mathbf{X}_\mathcal{R};\mathbf{Y}_2)$. Without loss of generality, we design a WNC–LDPC code at the SNR of -4 dB, where (1) the achievable sum rate of the source-to-relay MAC is 1; (2) the achievable sum rate of the source-to-destination MAC is 0.42; (3) the achievable rate of the relay at the destination is 0.86; (4) the achievable sum rate of the MARC is 0.6; and (5) the optimal time allocation t is 0.6. We also design a PNC–LDPC code at -4 dB, which is used as a benchmark for the WNC–LDPC code. According to various mutual information at -4 dB, our code rates are set as follows. Because the achievable sum rate of the source-to-relay MAC is 1, we set the code rate of each source as $R_i = 0.5$. The relay forwards the network-coded parity checks to the destinations with the code rate $R_\mathcal{R}$, which is set to 0.86. With the help of the relay, the achievable sum rate of the source-to-destination MAC is 0.42. Because the relay provides extra parity check digits, the codeword at the destination is the codeword transmitted by the sources concatenated by the extra parities from the relay. We call the code rate of the codeword at the destination as the equivalent code rate. That is, when decoding at the destination, the equivalent code rate of each source is $0.42/2 = 0.21$. We set $n = 25\,000$ in the BER simulations. Each source transmits $nt = 15\,000$ bits to the relay and the destination. Thus, each source has $ntR_i = 7500$ bits of information. The number of the extra network-coded parity checks provided by the relay is $(1-t)nR_\mathcal{R} = 8600$.

Next, after determining the code rates, we design the WNC–LDPC and the PNC–LDPC codes. In the WNC–LDPC code, we first need to determine the two sources' LDPC codes for the source-to-relay MAC. We adopt the two sources' LDPC codes for the source-to-relay MAC according to [16]. Then, with the two sources' codes, we optimise the network code at the relay according to our proposed method by using the EXIT analysis. The optimised degree distribution of the WNC–LDPC code is shown in Table I. In the PNC–LDPC code, the LDPC codes of the two sources for the source-to-relay channel are designed according to [10]. The code profiles are given as follows (edge perspective): $\lambda(x) = 0.161221x + 0.368766x^2 + 0.323428x^3 + 0.146585x^{19}$, $\rho(x) = 0.126096x^5 + 0.873904x^6$. Note that the relay only decodes $\mathbf{X}_1 \oplus \mathbf{X}_2$ and forwards $I(\mathbf{X}_\mathcal{R};\mathbf{Y}_2)$ bits of information to the destination. Here, we suppose that the relay forwards $I(\mathbf{X}_\mathcal{R};\mathbf{Y}_2)$ bits of the frame $\mathbf{X}_1 \oplus \mathbf{X}_2$ to the destination.

Figure 4 shows the BER curves for both the WNC–LDPC code and the PNC–LDPC code. In Figure 4, 'R, PNC–LDPC' denotes the BER at the relay of the PNC–LDPC code and 'D, PNC–LDPC' denotes the BER at the destination of the PNC–LDPC code. 'R, WNC–LDPC' and 'D, WNC–LDPC' are defined similarly. The BER at the

Table I. The degree distributions of the WNC-LDPC code from node perspective.

$v_{[0,1,0][a,b,0,0]}$	a	b	$v_{[0,0,1][0,0,c,d]}$	c	d	$\mu_{[a,b,c,d]}$	a	b	c	d
0.039919595241127	2	0	0.132588116799116	2	0	0.25	8	0	0	0
0.211438368243975	2	1	0.150279787338507	2	1	0.25	0	0	8	0
0.065659340484345	2	0	0.034149399831824	2	1	0.234432467117582	0	1	0	2
0.039124277470947	3	0	0.007015399696466	3	11	0.0307778081563195	0	2	0	1
0.061319148732688	3	1	0.125253294161907	3	1	0.024789724726099	0	2	0	2
0.053743265876906	3	0	0.021917998222167	3	0					
0.000445573234663	17	7	0.001540719662913	17	0					
0.001480315239234	17	4	0.002824418796263	17	7					
0.003063977836207	17	2	0.000624727850928	17	25					
0.005922101892882	18	0	0.004701782056931	18	0					
0.007755654675670	18	3	0.008643693823951	18	3					
0.005371502514347	18	6	0.005703783202017	18	2					
0.003050346217103	100	0	0.001829964112365	100	9					
0.001672741941386	100	1	0.001006291370321	100	25					
0.000033790398521	100	14	0.001920623074322	100	25					

Trans. Emerging Tel. Tech. **26**:380–388 (2015) © 2013 John Wiley & Sons, Ltd.
DOI: 10.1002/ett

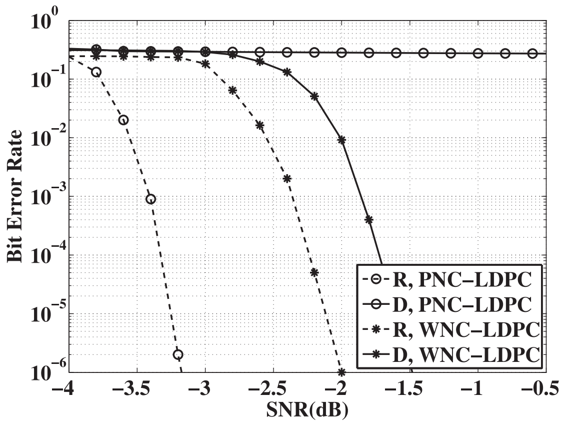

Figure 4. Bit error rate (BER) curves for PNC–LDPC and WNC–LDPC codes. SNR, signal-to-noise ratio.

relay of the PNC–LDPC code represents the BER of the frame $\mathbf{X}_1 \oplus \mathbf{X}_2$, because in the PNC, the relay can only decode $\mathbf{X}_1 \oplus \mathbf{X}_2$. In 'D, PNC–LDPC', 'R, WNC–LDPC' and 'D, WNC–LDPC', we calculate the average of the $\mathbf{X}_1$ and $\mathbf{X}_2$'s BERs. We can see from Figure 4 that the BER of 'R, PNC–LDPC' is much better than that of 'R, WNC–LDPC'. This is because in PNC–LDPC, the relay only needs to decode $\mathbf{X}_1 \oplus \mathbf{X}_2$, whereas in WNC–LDPC, the relay has to completely decode $\mathbf{X}_1$ and $\mathbf{X}_2$. However, in the PNC–LDPC, the BER at the destination is much worse than that in the WNC–LDPC. The BER of our WNC–LDPC code at the destination is 2.25 dB away from the capacity, whereas the BER of the PNC–LDPC code cannot converge at the whole SNR region. The reason for the poor performance of the PNC–LDPC code is as follows. The LLR values at the input of the destination decoder are calculated from the received signal $\mathbf{Y}_1 = h_{1\mathcal{D}}\mathbf{X}_1 + h_{2\mathcal{D}}\mathbf{X}_2 + \mathbf{N}_1$. Thus, in the BP decoding at the destination, $\mathbf{X}_i$ cannot obtain the extrinsic mutual information from network-coded bits $\mathbf{X}_1 \oplus \mathbf{X}_2$. Compared with the PNC–LDPC code, the network-coded bits in our WNC–LDPC code provide more extrinsic mutual information.

6. CONCLUSION

In this paper, we consider a MARC with two sources, one relay and one destination. We firstly derive the achievable rate region for the MARC with the WNC. Then, we propose a WNC–LDPC code structure based on the multi-edge type LDPC codes. An iterative detection-and-decoding receiver is used to deal with the multi-user interference at the destination. Finally, we optimise the WNC–LDPC code to approach the achievable rates by utilising the EXIT analysis. In the simulations, we consider a symmetric MARC, and our numerical results show that the BER performance of our WNC–LDPC code (with length 15 000 for each source) are 2.25 dB away from the capacity. Also, relative to the LDPC code optimised for the PNC, the WNC–LDPC code have a much better performance.

REFERENCES

1. Cover TM, Gamal AAE. Capacity theorems for the relay channel. *IEEE Transactions on Information Theory* September 1979; **25**(5): 572–584.
2. Kramer G, Gastpar M, Gupta P. Cooperative strategies and capacity theorems for relay networks. *IEEE Transactions on Information Theory* September 2005; **51**(9): 3037–3063.
3. Johnson SJ, Ong L, Kellett CM. Joint channel–network coding strategies for networks with low-complexity relays. *European Transactions on Telecommunications* November 2011; **22**(7): 396–406. DOI: 10.1002/ett.1492.
4. Militano L, Fitzek FHP, Iera A, Molinaro A. Network coding and evolutionary theory for performance enhancement in wireless cooperative clusters. *European Transactions on Telecommunications* December 2010; **21**(8): 725–737. DOI: 10.1002/ett.1435.
5. Hausl C. Joint network–channel coding for the multiple-access relay channel based on turbo codes. *European Transactions on Telecommunications* March 2009; **20**(2): 175–181. DOI: 10.1002/ett.1349.
6. Kim J, Park S, Kim J, Kim Y, Song H. Joint LDPC codes for multi-user relay channel, In *Fourth Workshop on Network Coding, Theory and Applications (NetCod)*, Hong Kong, China, January 2008; 1–6.
7. Youssef R, i Amat AG. Distributed turbo-like codes for multi-user cooperative relay networks, In *IEEE International Conference on Communications (ICC)*, Cape Town, South Africa, May 2010; 1–5.
8. Li J, Yuan J, Malaney R, Azmi MH, Xiao M. Network coded LDPC code design for a multi-source relaying system. *IEEE Transactions on Wireless Communications* May, 2011; **10**(5): 1538–1551.
9. Hatefi A, Visoz R, Berthet AO. Relaying functions for the multiple access relay channel, In *6th International Symposium on Turbo Codes and Iterative Information Processing (ISTC)*, Breast, France, September 2010; 364–368.
10. Zhang S, Liew S-C. Channel coding and decoding in a relay system operated with physical-layer network coding. *IEEE Journals on Selected Areas in Communincations* June 2009; **27**(5): 778–796.
11. Louie R, Li Y, Vucetic B. Practical physical layer network coding for two way relay channels: performance analysis and comparison. *IEEE Transactions on Wireless Communications* February 2010; **9**(2): 764–777.

12. Richardson TJ, Urbanke RL. Multi-edge type LDPC codes. Available Online: http://lthcwww.epfl.ch/papers/mutiledge.ps.
13. Brink S. Convergence behavior of iteratively decoded parallel concatenated codes. *IEEE Transactions on Communications* October 2001; **49**(10): 1727–1737.
14. Maunder RG, Hanzo L. Extrinsic information transfer analysis and design of block-based intermediate codes. *IEEE Transactions on Vehicular Technology* March 2011; **60**(3): 762–770.
15. Azmi MH, Yuan J. Design of multi-edge type bilayer-expurgated LDPC codes, In *IEEE International Symposium on Information Theory (ISIT)*, Seoul, Korea, June 2009; 1988–1992.
16. Roumy A, Declercq D. Characterization and optimization of LDPC codes for the 2-user Gaussian multiple access channel. *EURASIP Journal on Wireless Communications and Networking* 2007; **2007**: 10. DOI: 10.1155/2007/74890.
17. Storn R, Price K. Differential evolution—a simple and efficient adaptive scheme for global optimization over continuous spaces. *Technical Report TR-95-012, ICSI*, March 1995.